Electronic Supplementary Material (ESI) for Materials Chemistry Frontiers.
This journal is © the Partner Organisations 2019

Electronic Supplementary Information

Solid-Solid Interface Growth of Conductive Metal-Organic Framework Nanowire Arrays and Supercapacitor Application

Xing Du,[a] Jianing Zhang,[a] Huali Wang,[b] Zhaohui Huang,[b] Ankang Guo,[a] Lei Zhao,[a] Yue Niu,[c] Xianglong Li,[c] Bin Wu,[a] and Yunqi Liu*[a]*

[a]Beijing National Laboratory for Molecular Sciences, Key Laboratory of Organic Solids Institute of Chemistry, Chinese Academy of Science, Beijing 100190, P. R. China

E-mail: wubin@iccas.ac.cn; liuyq@iccas.ac.cn

[b]The State Key Laboratory of Refractories and Metallurgy, Wuhan University of Science and Technology, Wuhan 430081, P. R. China

[c]CAS Key Laboratory of Nanosystem and Hierarchical Fabrication, CAS Center for Excellence in Nanoscience, National Center for Nanoscience and Technology, Beijing 100190, P. R. China

This supporting information contains 16-page document, including 1 table, 13 figures, references and this cover page.

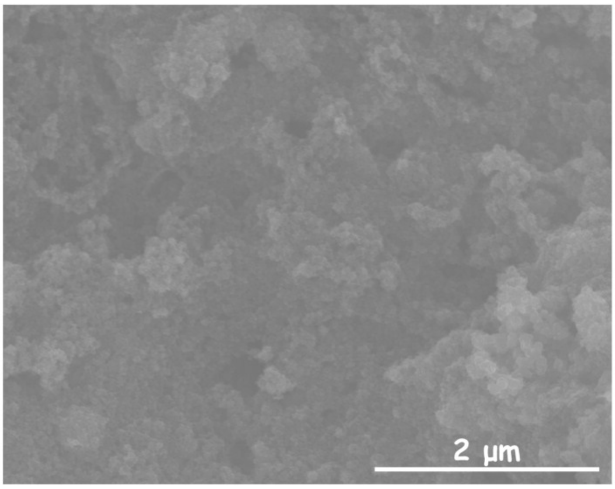

Figure S1. SEM image of $Cu_3(HHTP)_2$ crystallite powders synthesized by solvothermal method.

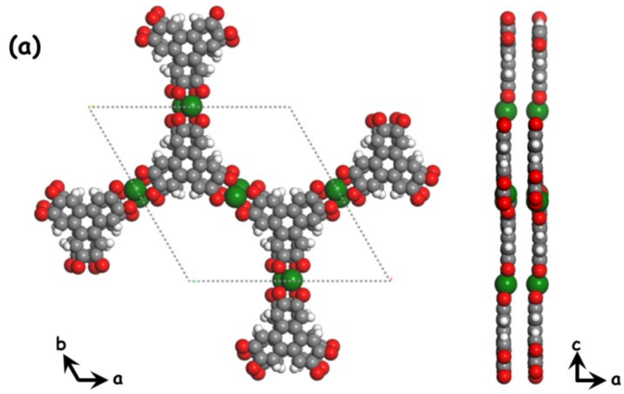

Space group	P6/mmm
a (Å)	21.3641
b (Å)	21.3641
c (Å)	6.7295
α (°)	90
β (°)	90
γ (°)	120

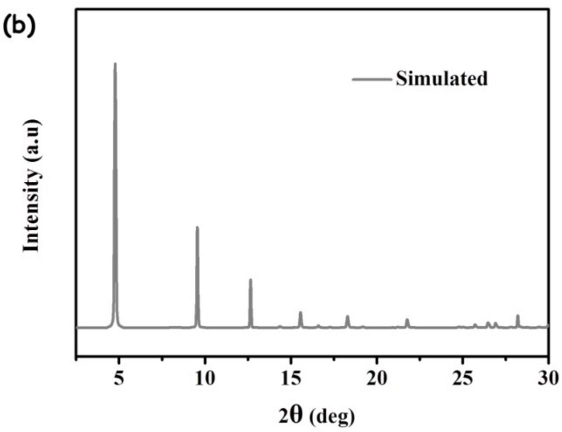

Range (°)	2~30
Step size (°)	0.0262606
X-ray source	Cu
λ_1	1.540598
λ_2	1.544426

Figure S2. (a) Top and side view of crystal structure and crystal data of $Cu_3(HHTP)_2$ in slipped-parallel (AB) packing mode. (b) Simulated powder X-ray diffraction (PXRD) spectrum pattern and simulated parameters of $Cu_3(HHTP)_2$.

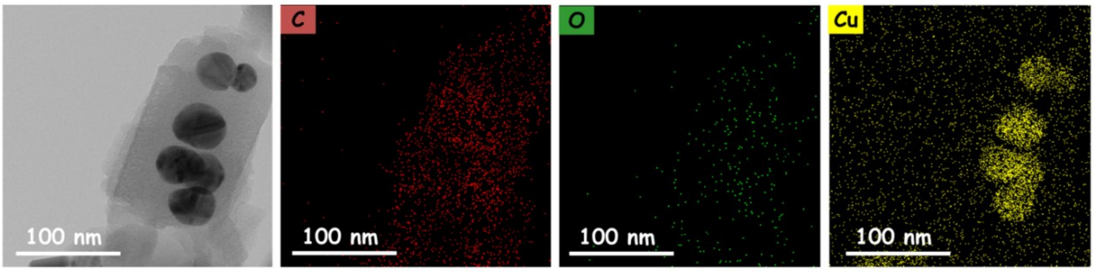

Figure S3. TEM image of $Cu_3(HHTP)_2$ nanowire after radiolysis, and elemental mapping images of carbon, oxygen and copper using TEM-EDS.

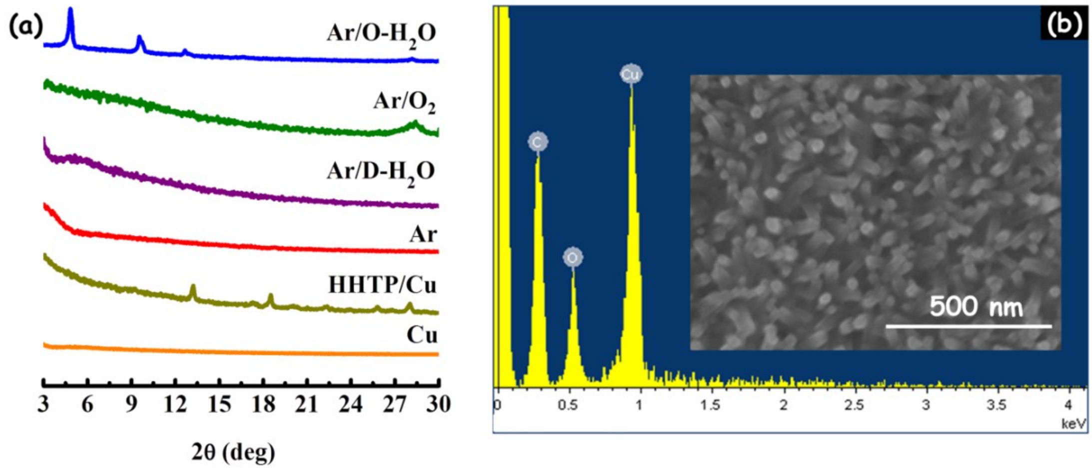

Figure S4. a) PXRD patterns of blank polished Cu foil, HHTP deposit on polished Cu foil, and products obtained under different conditions. b) SEM image (inset) and the corresponding EDS analysis of the product obtained under Ar/O_2 atmosphere.

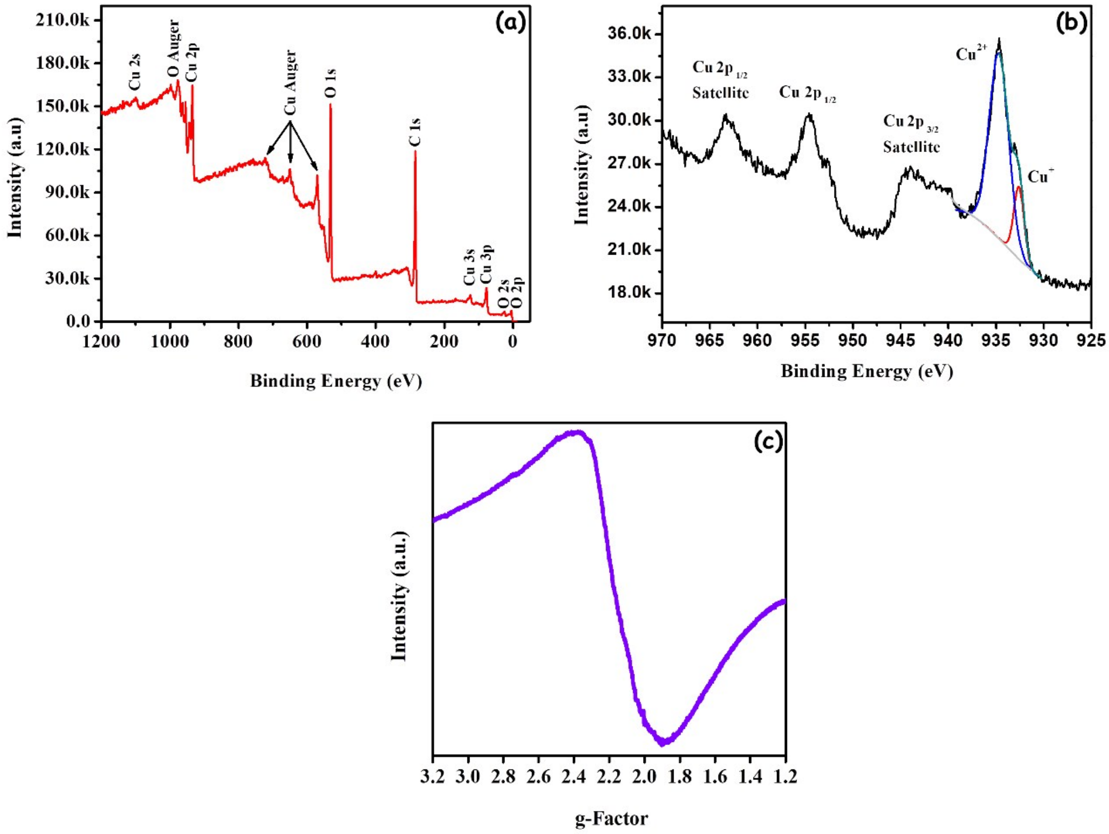

Figure S5. (a) Survey XPS spectra, (b) high-resolution Cu 2p XPS spectrum in which Cu $2p_{3/2}$ peak exhibits a dominant peak at ~935 eV for Cu^{2+} state and a weak peak at ~933 eV for Cu^{+} state, respectively, and (c) solid-state EPR spectrum recorded at room temperature of $Cu_3(HHTP)_2$ NWAs.

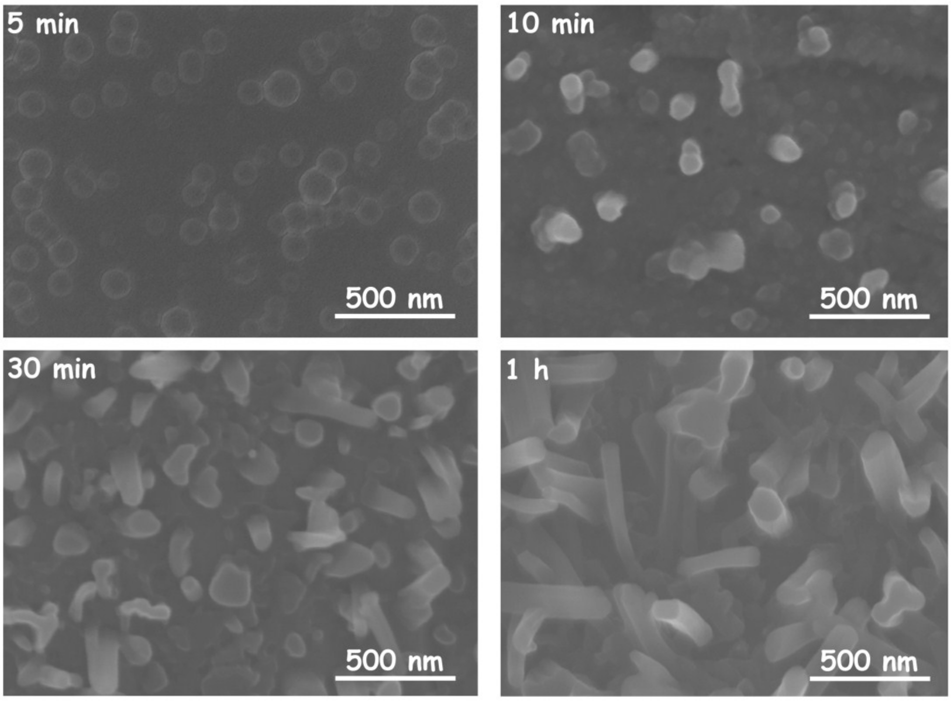

Figure S6. SEM images of the growth processes of $Cu_3(HHTP)_2$ nanowires on Cu foils. Different reaction time of 5 min, 10 min, 30 min and 1 h.

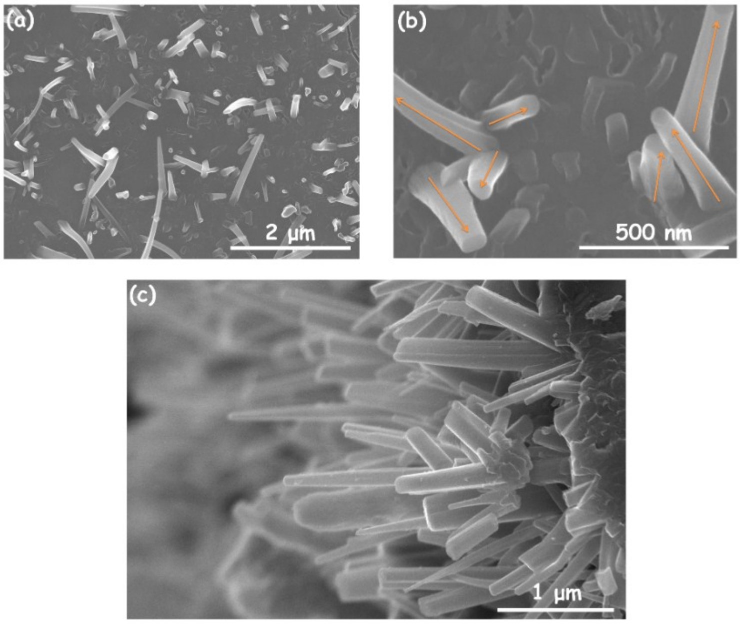

Figure S7. (a, b) SEM images of $Cu_3(HHTP)_2$ nanowires grown on Cu foils in the absence of restrictions. (c) A typical cross-section SEM image of as-grown sample indicating base-growth mode.

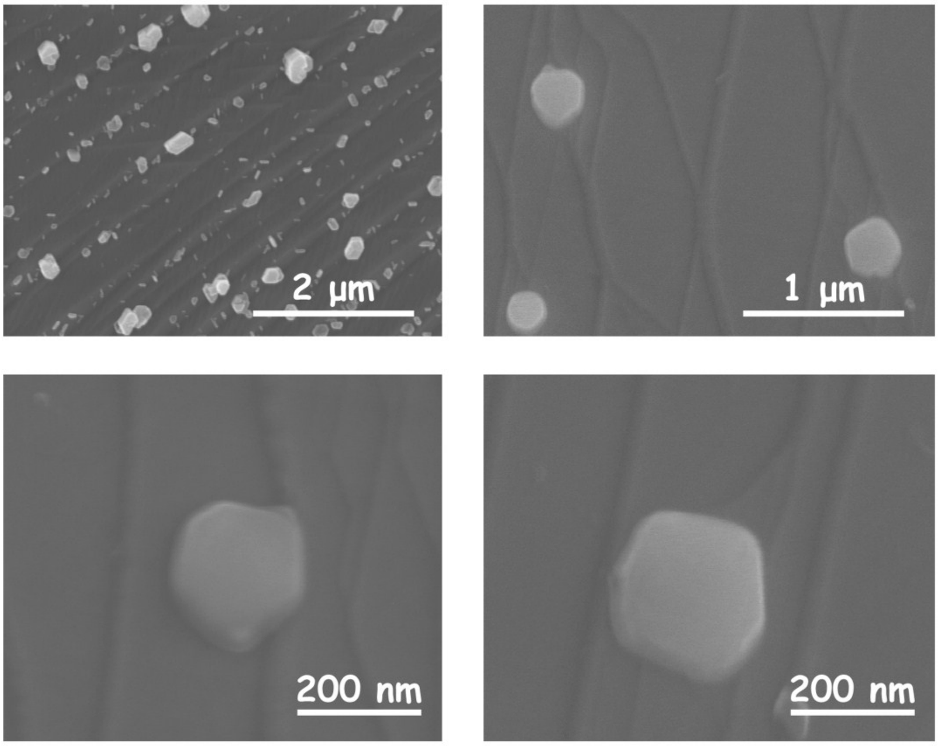

Figure S8. SEM images of $Cu_3(HHTP)_2$ grown on graphene/Cu foil. Note that MOFs crystals preferentially are grown along the Cu steps.

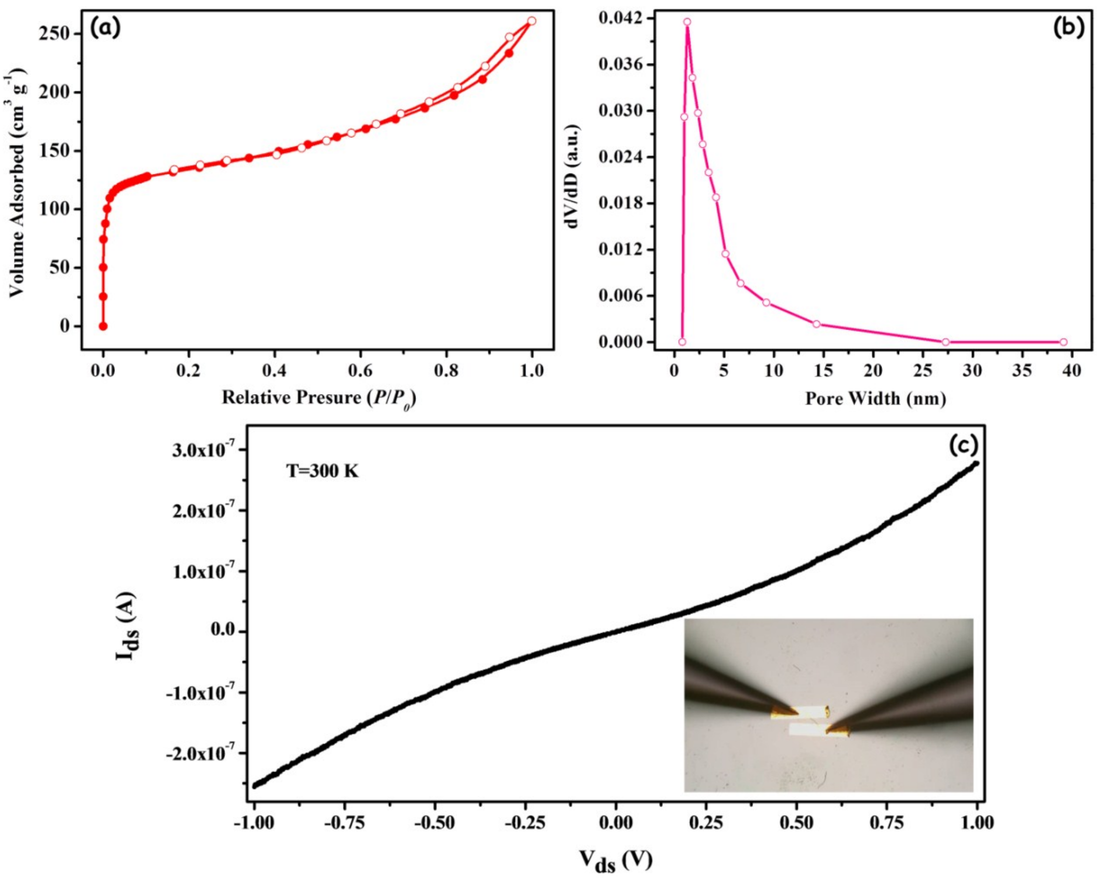

Figure S9. a) N_2 adsorption-desorption isotherms and b) pore size distribution of $Cu_3(HHTP)_2$ NWAs. c) Two-probe I-V curve of single $Cu_3(HHTP)_2$ nanowire. L =5 μm, W = 0.33 μm, H = 198 nm, Conductivity = 20.9 ± 2 S m^{-1}. Insert: photograph of the $Cu_3(HHTP_2)$ nanowire device used for conductivity measurement.

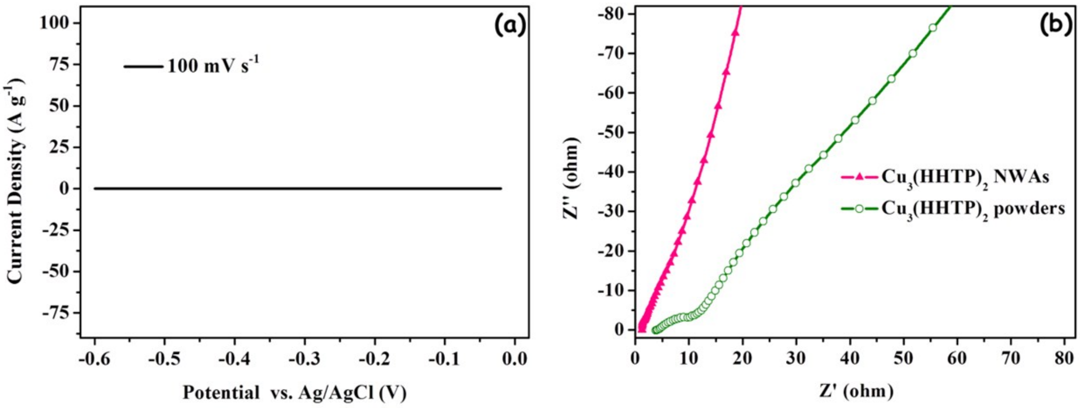

Figure S10. (a) CV curve of the current collector blank copper foil at -0.6V to -0.02V (vs. Ag/AgCl) at scan rate of 100 mV s^{-1}. (b) Nyquist electrochemical impedance spectra of $Cu_3(HHTP)_2$ NWAs and $Cu_3(HHTP)_2$ powders.

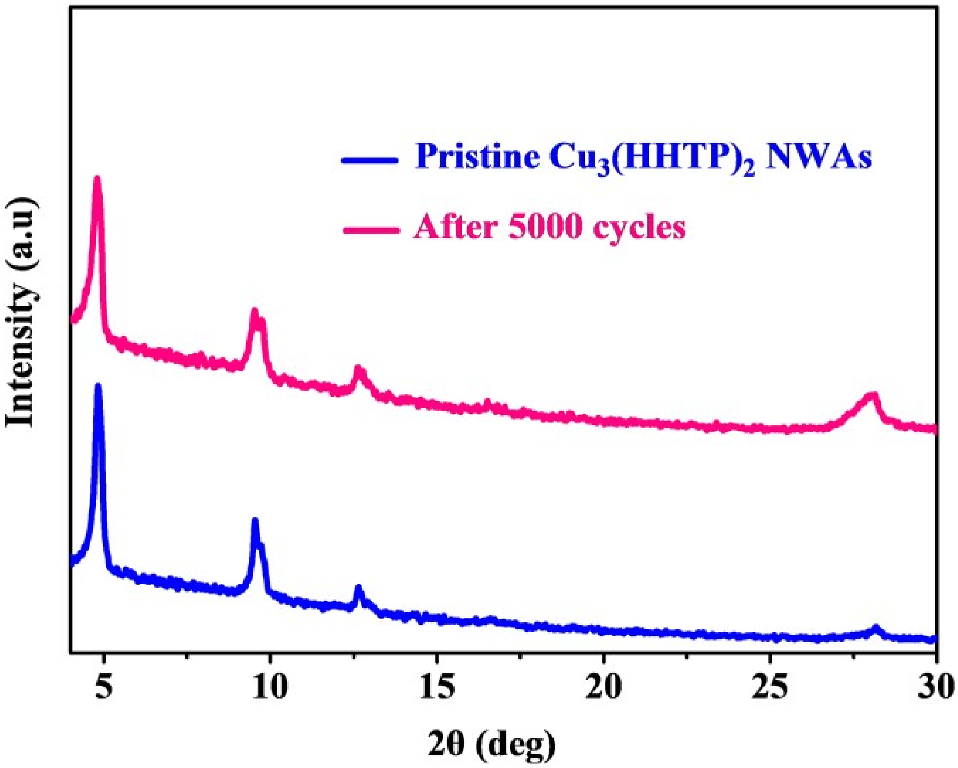

Figure S11. PXRD of $Cu_3(HHTP)_2$ NWAs/Cu electrodes before and after 5000 cycles.

Table S1. Performance comparison of symmetric supercapacitors based on $Cu_3(HHTP)_2$ NWAs and carbon materials.

Materials	Specific capacitance F g^{-1} (Conditions)	Aqueous electrolyte	Normalized capacitance μF cm^{-2} (BET SSA[a)],m^2 g^{-1})	Reference
$Cu_3(HHTP)_2$ NWAs	195.3 (0.5 A g^{-1})	1 M KCl	41.1 (475)	This work
Microporous carbons	22~204 (0.05 A g^{-1})	2 M H_2SO_4	7.6~22.4 (250~2298)	[1]
N-doped carbon nanocages	313 (1.0 A g^{-1})	6 M KOH	17.4 (1794)	[2]
N-doped carbon capsules	240 (0.1 A g^{-1})	1 M H_2SO_4	16 (1500)	[3]
Single-walled carbon nanotubes	140 (0.01A g^{-1})	6 M KOH	21.7 (644)	[4]
Single-walled carbon nanohorns	66 (0.001 A cm^{-2})	1 M H_2SO_4	22.7 (291)	[5]
thermal exfoliation graphene	117 (100 mV s^{-1})	1 M H_2SO_4	12.6 (925)	[6]
Graphene/carbon nanotube	290.4 (0.5 A g^{-1})	1 M KCl	68.9(421.3)	[7]

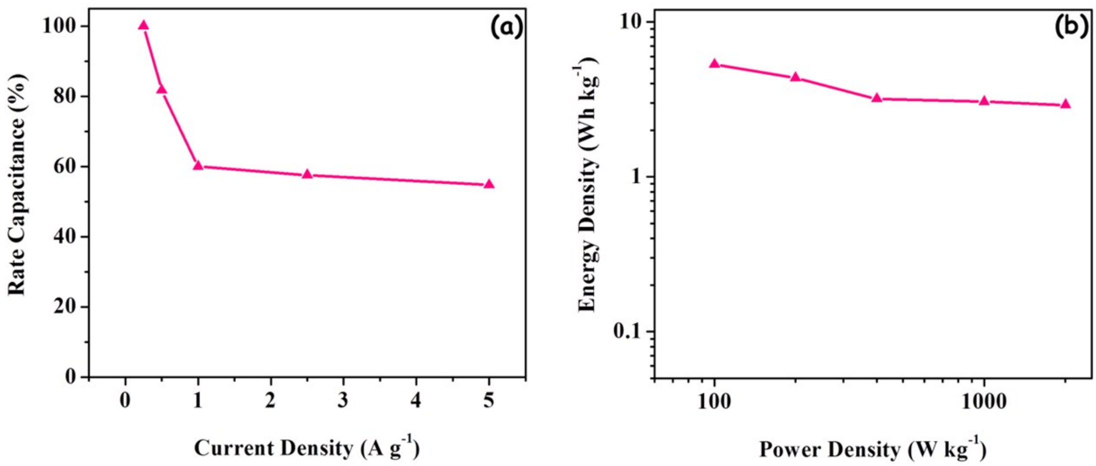

Figure S12. (a) The rate performance of symmetric supercapacitor based on $Cu_3(HHTP)_2$ NWAs at current density from 0.25 to 5 A g^{-1}. (b) Ragone plot of symmetric supercapacitor based on $Cu_3(HHTP)_2$ NWAs.

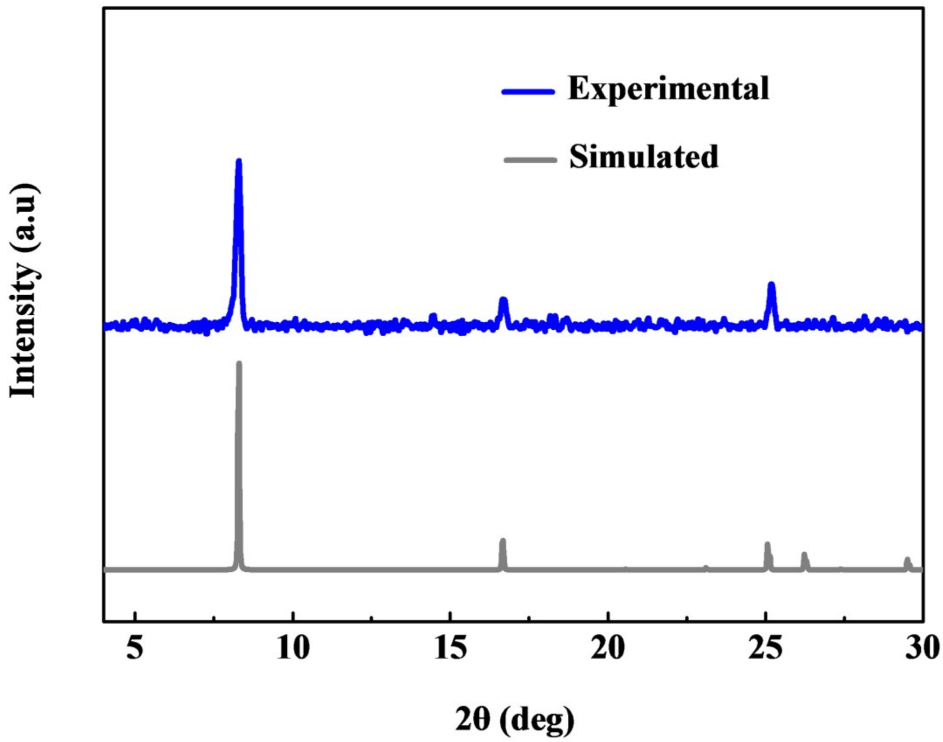

Figure S13. Experimental and simulated PXRD patterns of $Fe_3(HHB)_2$. Experimental conditions: The hexahydroxybenzene (HHB) was located at the high temperature zone of the furnace. The pretreated Fe foils were placed in another quartz boat, and then located at the downstream of the low temperature zone of the furnace. The chamber was evacuated to 1 Torr. Then, the temperature of high temperature zone was gradually increased to 250 °C (25 °C/min) and maintained for 60 min. After that, the low temperature zone is heated to 100 °C and kept for a period of time with argon/oxygenated water (Ar/O-H_2O) mixtures flow of 10 sccm to form $Fe_3(HHB)_2$.

REFERENCES

1 W. H. Li, K. Ding, H. R. Tian, M. S. Yao, B. Nath, W. H. Deng, Y. Wang and G. Xu, *Adv. Funct. Mater.*, 2017, **27**, 1702067-1702074.

2 T. A. Centeno and F. Stoeckli, *Electrochim. Acta*, 2011, **56**, 7334-7339.

3 J. Zhao, H. Lai, Z. Lyu, Y. Jiang, K. Xie, X. Wang, Q. Wu, L. Yang, Z. Jin, Y. Ma, J. Liu and Z. Hu, *Adv. Mater.*, 2015, **27**, 3541-3545.

4 G. A. Ferrero, A. B. Fuertes and M. Sevilla, *J. Mater. Chem. A*, 2015, **3**, 2914-2923.

5 F. Picó, J. M. Rojo, M. L. Sanjuán, A. Ansón, A. M. Benito, M. A. Callejas, W. K. Maser and M. T. Martínez, *J. Electrochem. Soc.*, 2004, **151**, A831-A837.

6 C. M. Yang, Y. J. Kim, M. Endo, H. Kanoh, M. Yudasaka, S. Iijima and K. Kaneko, *J. Am. Chem. Soc.*, 2007, **129**, 20-21.

7 S. R. C. Vivekchand, C. S. Rout, K. S. Subrahmanyam, A. Govindaraj and C. N. R. Rao, *J. Chem. Sci.*, 2008, **120**, 9-13.

8 Q. Cheng, J. Tang, J. Ma, H. Zhang, N. Shinya and L. C. Qin, *Phys. Chem. Chem. Phys.*, 2011, **13**, 17615-17624.